

# Pressure Profile Estimation through CFD in UBD Operation Considering with Influx to Wellbore

**Dabiri Atashbeyk, Meysam; Shahbazi, Khalil**

*Department of Petroleum Engineering, Ahwaz Faculty of Petroleum Engineering,  
Petroleum University of Technology, Abadan, I.R. IRAN*

**Fattahi, Moslem\*<sup>+</sup>**

*Department of Chemical Engineering, Abadan Faculty of Petroleum Engineering,  
Petroleum University of Technology, Abadan, I.R. IRAN*

**ABSTRACT:** Nowadays, UnderBalanced Drilling (UBD) technology is widely applicable in the petroleum industry due to its advantages to an overbalanced drilling operation. UBD success depends on maintaining the drilling fluid circulating pressure below the reservoir pore pressure during operations. One of the main prerequisites of a successful UBD operation is the correct estimation of the pressure profile. In this investigation, the pressure profile was obtained with consideration of the influx to the wellbore. A spreadsheet was developed to obtain the pressure profile using an analytical solution for aerated mud in UBD operation. Moreover, a numerical simulation was employed to simulate the three-phase flow in annulus through the UBD operation and the transient Eulerian model flow via the turbulence  $k-\epsilon$  model. The effects of solid particle size and rotation of the inner pipe were considered on the pressure drop. It was observed that pressure drop was significantly increased with increasing solid particle size while it remained almost constant with increasing of the inner pipe rotation. The analytical and numerical results were compared with published experimental results and showed a good agreement.

**KEYWORDS:** Underbalanced drilling; Pressure profile; Transient flow; CFD technique.

## INTRODUCTION

Underbalanced drilling (UBD) is the drilling process in which the wellbore pressure is intentionally designed to be lower than the pressure of the formation being drilled. This underbalanced pressure condition allows the reservoir fluids to enter the wellbore during drilling, thus, several other significant benefits that are superior to conventional drilling techniques. These include the increasing

preventing fluid loss and related causes of formation damage. As a result, special additional equipment and procedures are required before, during, and after a UBD operation. In addition to improving well productivity by preventing fluid loss and formation damage, UBD offers of penetration rate and bit life, reduced probability of sticking the drill string downhole and improving

---

\* To whom correspondence should be addressed.

+ E-mail: [fattahi@put.ac.ir](mailto:fattahi@put.ac.ir)

1021-9986/2018/6/271-283

13/\$/6.03

the formation evaluation [1, 2]. UBD advantages and disadvantages should be juxtaposed so that an appropriate decision can be made in terms of UBD feasibility in a specified region. Experience has indicated that in the right circumstances, significant technical and economic benefits can be obtained when care is taken in the design of a UBD program [3, 4].

Because of the naturally fractured nature of most Iranian reservoirs, such as the Asmari and Bangestan formations, UBD technology is more beneficial for these depleted reservoirs [4]. Although it is more beneficial to use UBD because of these advantages, formation damage mitigation is, unfortunately, not the first priority in Iran. This is due to imprecise pressure prediction and insignificant pressure control.

Since UBD conditions in subnormal pressure formations frequently require the simultaneous injection of a mixture of liquid and gas circulating as a two phase flow, multiphase flow knowledge is required inside the drill string and in the annulus along the circulating path. The flow returning to the surface consists of a compressible multiphase mixture including the formation and injected fluids as well as drilled cuttings [2].

During UBD operation, gas and liquid are pumped simultaneously from the surface down through the drill string, through the bit and then up to the annulus. Based on pressure, temperature and geometry variation during the circulating flow path, different flow patterns occur. Study of the physics of two phase flow in a mud circulating path has resulted in several mechanistic models for different flow patterns.

Estimation of Bottom Hole Pressure (BHP) during the drilling operation is the most important task in UBD design. This task is difficult due to the complex nature of the multiphase flow in the UBD system, especially in the annulus between the drill pipe, collars and the wellbore where water, gas, cuttings and fluid influx from the penetrated formations are presented. To accomplish this task, the BHP should be calculated. Nonetheless, the BHP, fluid influx flow rates, as well as fluid properties along the wellbore are interdependent parameters that can only be derived through a combination of iterative and finite difference methods.

Computational Fluid Dynamics (CFD) has presented an effective tool for accomplishing this objective because of its ability to simulate the heat and mass transfer,

as well as mixing and related phenomena involving turbulence [5].

Experimental study of cuttings transport with air-water mixtures for horizontal and highly-inclined wellbores was conducted by *Vieira et al.* [6]. His study represented that the cuttings were carried by the liquid phase only and offered a minimum air-water combination required to prevent a stationary bed, which developed at the intermittent boundary of the flow pattern map [6].

*Rodriguez* (2001) performed an experimental study to find the minimum air and water flow rates that effectively transport cuttings through highly inclined and horizontal wells. The experiments were carried out in a low pressure field scale flow loop [7].

Minimum air and water flow rates required for effective cuttings transport in high angle and horizontal wells were studied by *Vieira et al.* (2002). Extensive experiments were performed in a unique field-scale low-pressure flow loop. The effects of gas and liquid flow rates, drilling rate, inclination angle, pressure drop and flow patterns on cuttings transport were investigated [8].

The mechanism of cutting transport in UBD through the modeling was performed by *Doan et al.* (2003). The model simulated the transport of drill cuttings in an annulus of arbitrary eccentricity. Besides, a wide range of transport phenomena including cuttings deposition as well as re-suspension, formation, and movement of cuttings bed were studied. The model consists of conservation equations for the fluid and cuttings components in the suspension and the cuttings deposit bed [9].

A mechanistic model for UBD with aerated muds was developed by *Zhou et al.* (2005). The hydraulic model determined the flow pattern and frictional pressure loss in a horizontal concentric annulus. The influences of Gas Liquid Ratio (GLR) and other flow parameters on frictional pressure loss were analyzed using the developed model [10].

The analysis of two sets of experiments was performed at PETROBRAS real scale facility aiming to evaluate of solids return times in aerated fluids [11]. Furthermore, in this investigation, the effect of liquid and gas injection rates, particle diameter, liquid phase viscosity and annular back pressure on the transport capacity of solids in a vertical well with aerated water and polymer-based drilling fluids were studied [11, 12].

A mechanistic model for cuttings transport by combining two-phase hydraulic equations, turbulent boundary layer theory, and particle transport mechanism was developed by Zhou (2008). Effects of temperature, bottom hole pressure, liquid flow rate, gas injection rate, cuttings size and density, inclination angle, and rheological properties of drilling mud on hole cleaning were analyzed. The model was validated by available experimental data [13].

In UBD, the concept of primary good control (containing the formation fluids by means of hydrostatic columns greater than the formation pressure) is replaced by the concept of flow control. In flow control, the BHP and influx of formation fluids must be controlled. Therefore, in UBD operations the BHP must be maintained between two pressure boundaries which define the UBD pressure window [14].

It is accepted that the success of a UBD operation is a function of the ability to maintain underbalanced conditions during the entire drilling process. Unfortunately, during jointed-pipe drilling, the surface injection must be interrupted every time a connection or trip is needed. This stopping of injection causes the disruption of steady state conditions.

Besides, if the BHP fluctuations are not properly maintained below the formation pressure, the formation is exposed to an overbalanced condition every time a connection or trip takes place. These periods of overbalanced can ruin or reduce the advantages obtained after making the efforts and expenses to drill the well underbalanced [15]. This problem is often compounded by the fact that very thin, low viscosity base fluid systems are usually utilized in most UBD operations.

From a practical engineering point of view, one of the major design difficulties in dealing with the multiphase flow is that the mass, momentum, and energy transfer rates and processes can be quite sensitive to the geometric distribution or topology of the components within the flow [16]. An appropriate starting point is a phenomenological description of the geometric distributions or flow patterns that are observed in common multiphase flows.

The definition of the flow regime is a description of the morphological arrangement of the components or flow pattern [17]. It is important to appreciate that different flow regimes occur at different fluid flow rates and differences also occur for different materials.

Multiphase flow regimes can be grouped into four categories: gas-liquid or liquid-liquid; gas-solid; liquid-solid and three-phase flows [18]. Three-phase flows are combinations of the other flow regimes. This means a combination of gas-liquid-solid or two solid phases and one gas phase, etc. These types of flow can be seen at a petroleum refinery, in chemical separation technology or in combustion.

Modeling and simulation of gas-liquid two-phase flow in UBD operation in order to predict the BHP and other parameters of two-phase flow were performed. Through the one-dimensional steady-state, two-fluid model in the Eulerian frame was used to simulate the two-phase flow in the UBD operation. The parameters such as pressure, volume fraction and velocities of two phases at different flow regimes, namely bubbly, slug and churn turbulent flow were predicted [19]. Reduced Order Modeling (ROM) of transient two-phase flow in the UBD operation using Proper Orthogonal Decomposition (POD) method in the annulus of the drilling well was applied. The employed POD approach reduced the required CPU-time as much as 62% [20]. Gas-Liquid-Solid three-phase flow in the annulus of a well with industrial dimensions was simulated numerically by the multi-fluid approach at UBD operations. The comparisons showed that three-phase numerical simulation gives better accuracy compared to two-phase numerical simulation and most of the other mechanistic models. Moreover, the effects of controlling parameters such as liquid and gas flow rate, drilling rate, size of cuttings and choke pressure on the BHP were investigated [21].

This work presents a CFD simulation to predict pressure by coupling drilling and inflow performance parameters such as gas injection rates, liquid flow rates and fluid production rates for UBD. A concentration on both two-phase flow and three-phase flow regimes are the objective of this study.

### *CFD technique*

CFD is the science of predicting fluid flow, heat transfer, mass transfer, chemical reactions, and related phenomena by solving the mathematical equations which govern these processes using numerical methods and algorithms [22]. In order to provide easy access to their solving power, all commercial CFD packages include sophisticated user interfaces to input problem parameters and to examine the results.

In CFD, equation discretization is usually performed using the Finite Difference Method (FDM), the finite element method (FEM) or the finite volume method (FVM) [23]. Spatial discretization divides the computational domain into small sub-domains making up the mesh. The fluid flow is described mathematically by specifying its velocity at all points in space and time. All meshes in CFD comprise nodes at which flow parameters are resolved. The three main types of meshes commonly used in computational modeling are structured unstructured and multi-block structured meshes.

It is important to include turbulence in the study of multiphase flow. Various closure models of turbulence are available to describe and solve the effects of turbulent fluctuations of velocities and scalar quantities of flow. In comparison to single-phase flows, the number of terms to be modeled in the momentum equations in multiphase flow is large, and this makes the modeling of turbulence in multiphase simulations extremely complex [24].

In the present work, the Eulerian-Granular approach is employed to simulate the three-phase flow (water-gas-solid) in the annulus. This multiphase model solves the momentum and continuity equations for each phase. The following continuity equations are utilized to calculate the volume fraction of each phase [25].

Continuity equation for gas phase:

$$\frac{\partial}{\partial t}(\alpha_g \rho_g) + \nabla \cdot (\alpha_g \rho_g \vec{V}_g) = 0 \quad (1)$$

Continuity equation for solid phase:

$$\frac{\partial}{\partial t}(\alpha_s \rho_s) + \nabla \cdot (\alpha_s \rho_s \vec{V}_s) = 0 \quad (2)$$

Continuity equation for liquid phase:

$$\frac{\partial}{\partial t}(\alpha_l \rho_l) + \nabla \cdot (\alpha_l \rho_l \vec{V}_l) = 0 \quad (3)$$

The momentum equations for gas, solid and liquid phase are defined as follows.

Momentum equation for gas phase:

$$\frac{\partial}{\partial t}(\alpha_g \rho_g \vec{V}_g) + \nabla \cdot (\alpha_g \rho_g \vec{V}_g \vec{V}_g) =$$

$$-\alpha_g \nabla p + \nabla \cdot \vec{\tau}_g + \alpha_g \rho_g \vec{g} + K_{gs}(\vec{V}_g - \vec{V}_s) + K_{gl}(\vec{V}_g - \vec{V}_l)$$

Momentum equation for solid phase:

$$\frac{\partial}{\partial t}(\alpha_s \rho_s \vec{V}_s) + \nabla \cdot (\alpha_s \rho_s \vec{V}_s \vec{V}_s) =$$

$$-\alpha_s \nabla p - \nabla p_s + \nabla \cdot \vec{\tau}_s + \alpha_s \rho_s \vec{g} + K_{gs}(\vec{V}_g - \vec{V}_s) +$$

$$K_{sl}(\vec{V}_l - \vec{V}_s) + (\vec{F}_s + \vec{F}_{lift,s} + \vec{F}_{vm,s})$$

Momentum equation for liquid phase:

$$\frac{\partial}{\partial t}(\alpha_l \rho_l \vec{V}_l) + \nabla \cdot (\alpha_l \rho_l \vec{V}_l \vec{V}_l) =$$

$$-\alpha_l \nabla p + \nabla \cdot \vec{\tau}_l + \alpha_l \rho_l \vec{g} + K_{gl}(\vec{V}_g - \vec{V}_l) + K_{sl}(\vec{V}_s - \vec{V}_l)$$

Where s, g and l are the representative indexes for solid, gas, and liquid phases, respectively. Moreover,  $\alpha$  is the volume fraction,  $g$  is the acceleration of gravity,  $\rho$  is the density,  $\tau$  is the stress tensor and  $\vec{V}$  is the velocity. The expression that represented the stress tensor for gas, solid and liquid phase, as well as the other related parameters, were obtained from references [26-29].

In the present work, ANSYS FLUENT 12.1 software package was utilized. It provides three methods for modeling turbulence in multiphase flows within the context of the  $\kappa$ - $\epsilon$  models. In addition, there are two turbulence options within the context of the Reynolds Stress Models (RSM).

## THEORITICAL SECTION

### Model description

Three phase flow (Air-Water-Cutting) experiment performed by Osgouei

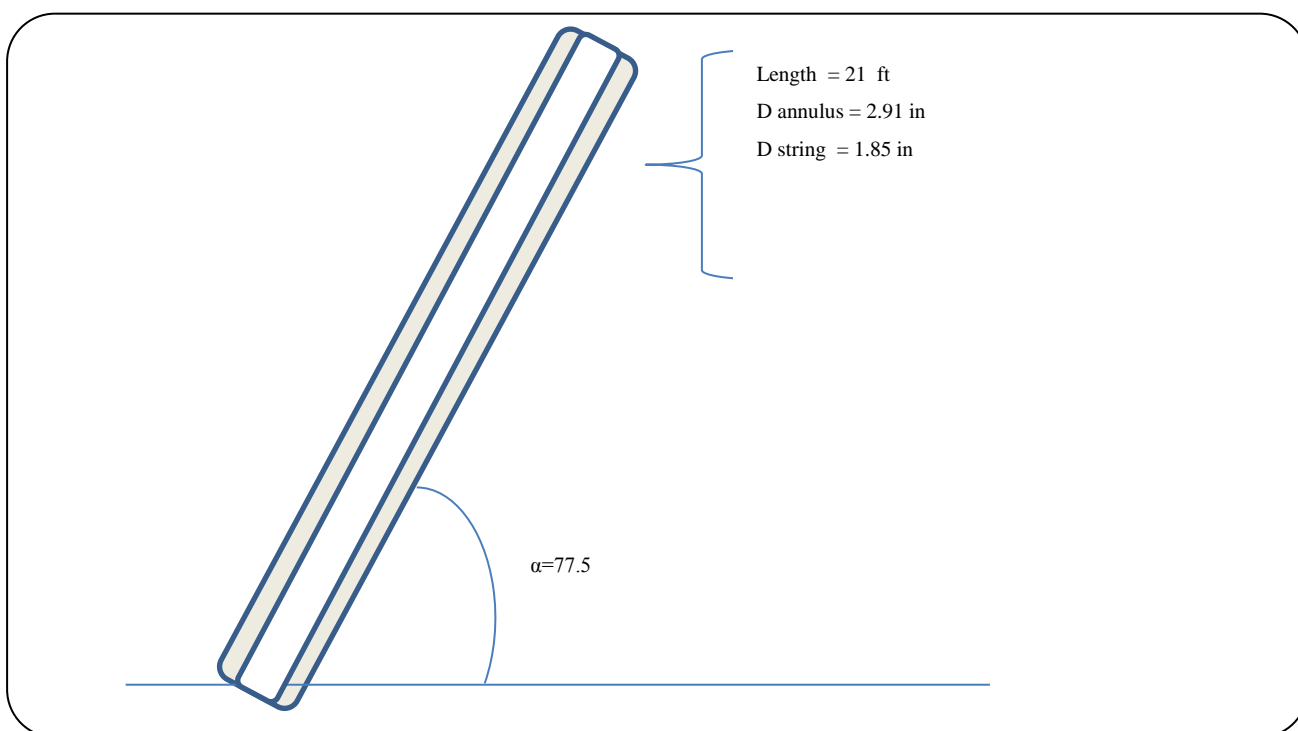
Fig. 1 shows a two dimensional overview of the model (eccentric annulus) in this study.

Table 1 shows the three phases flow experimental data utilized in this simulation. Standard experimental procedures adapted for three-phase flow were as follows: the liquid was pumped at a constant flow rate using a centrifugal pump. Then, the air was introduced at the desired rate. Once both the air and liquid flow rates were stabilized, the cutting was injected from an injection tank into the system. When the cutting, gas and liquid flow rates were stable, the data acquisition was activated in order to record flow rates, pressures at critical points, pressure drop inside the test section, etc. [30].

The physical model is an eccentric annulus with two ends. One is the entrance of solid-liquid-gas three-phase flow, and the other is the outlet. The drillpipe is located inside the annulus, and the effect of the joint is neglected.

**Table 1: Three-phase flow experimental data for an inclined (77.5° from horizontal) eccentric annulus Cutting-Gas-Water flow obtained from Ref. [30].**

Mud Superficial Velocity (m/s)	Gas Superficial Velocity (m/s)	Pressure Transmitter (psig)	ROP (ft/hr)	Pressure Gradient (psi/ft)
1.5338	0.6767	5.162	80	0.461
1.545	1.2308	5.137	80	0.440
1.5277	1.8721	5.034	80	0.425
1.5243	2.592	5.001	80	0.417
1.5618	3.2275	5.063	80	0.421



**Fig. 1: Two dimensional overview of the model.**

The inner boundary conditions are set to be rotational one and the outer boundaries are the good walls.

The problem comprises a three-phase flow in an annulus in which air and water enter at the bottom of the annulus. Table 2 shows the properties of air, water and solid used [30].

#### **Steady state three-phase flow simulation**

In the present work, a Eulerian model has been chosen to simulate three-phase flow in an eccentric annulus. We have used a steady approach for all simulations except one where we used an unsteady approach. Brief details of the simulations are as follows:

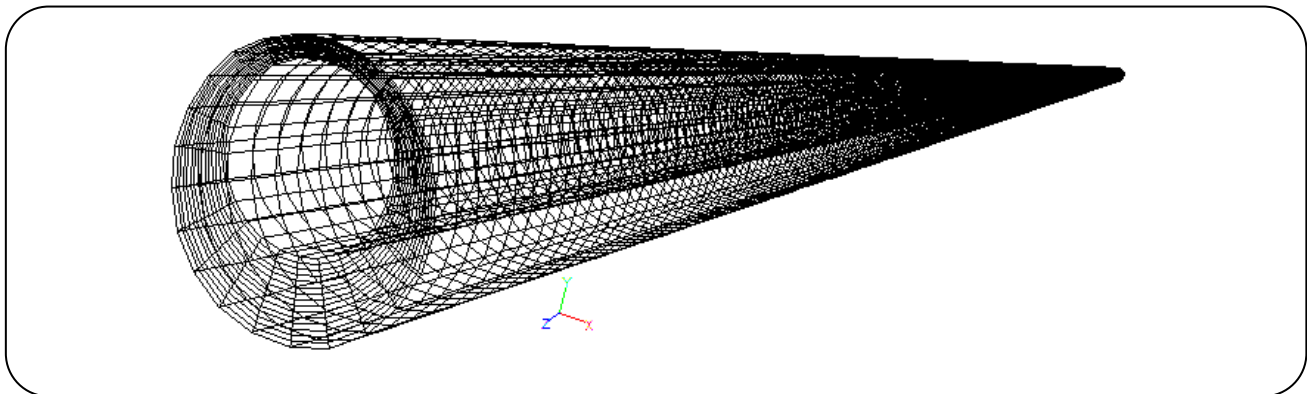
#### **Meshing**

Determining a mesh was an important step towards solving the three-phase flow problem. ANSYS FLUENT was chosen as the solver. Relevance qualitatively defines the fineness of the mesh and incorporates additional quantitative conditions that need to be specified.

The sizing category was set with maximum cell squish of 0.0876117, the maximum aspect ratio of 19.2143 and cell numbers of 139656. The advanced sizing features added complexity to the problem that was not needed and resulted in a less-uniform mesh overall. The relevance center was specified as “fine” to increase the uniformity overall. Mesh uniformity was important for

**Table 2: Properties of air, water, and solid used in the current study.**

Phase	Density (kg/m <sup>3</sup> )	Viscosity (kg/m.s.)
Air	1.225	$1.789 \times 10^{-5}$
Water	998.2	$1.003 \times 10^{-3}$
Solid	2470	-

**Fig. 2: Isometric view of mesh for this model.**

this research because meshes with high uniformity can be used to lead to more accurate results.

#### *Choosing a general multiphase model*

The first step in solving any problem is to determine which of the regimes provides some broad guidelines for determining the degree of inter-phase coupling for flows involving bubbles, droplets, or particles and the appropriate model for different amounts of coupling. The appropriate model for flows involving, bubbles, particles or droplets are as follows [31]:

- For bubble, droplet and particle-laden flows in which dispersed-phase volume fractions are less than or equal to 10% the discrete phase model to be used.
- For bubble, droplet and particle-laden flows in which the phases mix and/or dispersed phase volume fractions exceed 10% the mixture model is used.
  - For slug flow, the VOF model is used.
  - For stratified/free-surface flows, the VOF model is used.
  - For the fluidized bed, the Eulerian Model for granular flow is used.
  - For slurry flows and hydro transport, the Eulerian or mixture model is used.

A 3D segregated, first order implicit steady state solver was used. The standard k-ε dispersed Eulerian

multiphase model with standard wall functions was used for turbulence modeling. Water was taken as the primary phase which is the continuous phase, while solid and air are as the dispersed phase. Inter-phase interaction formulations used for drag coefficient were as follows [32]:

- Air-Water: Schiller-Naumann
- Solid-Water: Gidaspow
- Solid-Air: Gidaspow

Air velocities ranging from 0.6767 m/s to 3.2275 m/s and water velocities from 1.5338 to 1.5618 m/s were used, respectively. The inlet air volume fraction was obtained as the fraction of air entering in the mixture of gas and liquid. It is noteworthy that backflow granular temperature specifies temperature for the solids phase and is proportional to the kinetic energy of the random motion of the particles.

Pressure outlet boundary conditions:

Mixture gauge pressure= 0 Pa

Solid and liquid boundary conditions:

Backflow granular temperature=  $0.0001 \text{ m}^2/\text{s}^2$

Backflow volume fraction= 0

#### *The solution of steady state three-phase flow*

The under relaxation factor for solution control in different flow quantities were taken as; Pressure=0.3,

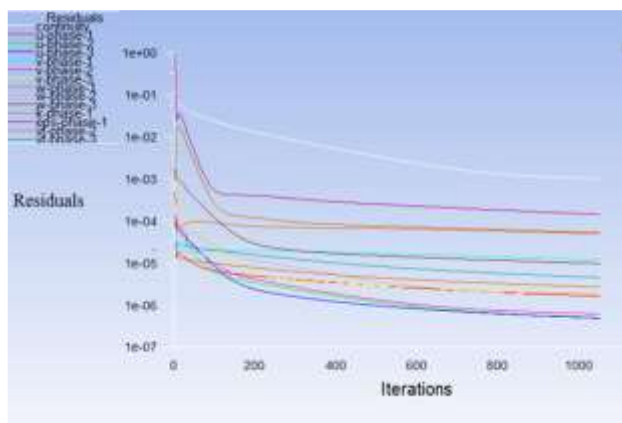


Fig. 3: Plot of residuals for the  $k-\epsilon$  solver method as the iteration proceeds.

Density=1, Body forces=1, Momentum=0.3, Volume fraction=0.5, Granular temperature=0.2, Turbulent kinetic energy=0.8, Turbulent dissipation rate=0.8, Turbulent viscosity=1. Pressure-velocity coupling was chosen as a phase coupled SIMPLE. First order upwind was chosen for discretization. The solution has been initialized from all zones. For patching a solid volume fraction, the volume fraction of the solid in the part of the column up to which the solid was fed, was used. Fig. 3 shows the residual plot for the  $k-\epsilon$  solver method as the iteration proceeds.

#### Transient three-phase flow simulation

A 3D segregated first order implicit unsteady solver was utilized. Air velocity of 0.6767 m/s and water velocity of 1.5338 m/s were used.

Pressure outlet boundary conditions:

Mixture gauge pressure= 0 Pa

Solid and liquid boundary conditions:

Backflow granular temperature=  $0.0001 \text{ m}^2/\text{s}^2$

Backflow volume fraction= 0

#### The solution of transient three-phase flow simulation

The under relaxation factor for solution control in different flow quantities were taken as; Pressure=0.3, Density=1, Body forces=1, Momentum=0.3, Volume fraction=0.5, Granular temperature=0.2, Turbulent kinetic energy=0.8, Turbulent dissipation rate=0.8, Turbulent viscosity=1. The formation of water, oil, and gas influx rates were 22.18, 88.72 and 739.34 bbl/h, respectively. Pressure-velocity coupling was chosen as a phase coupled

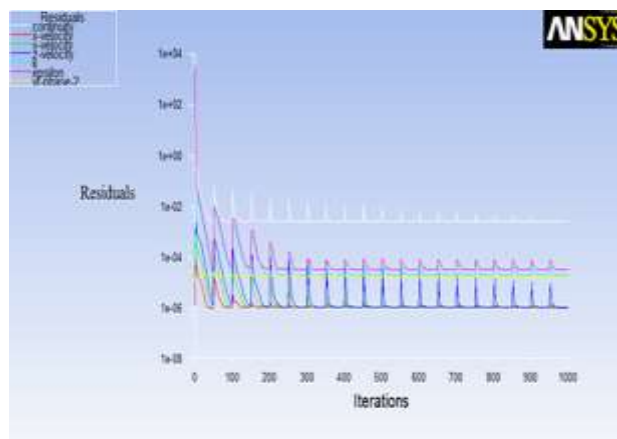


Fig. 4: Residuals for the  $k-\epsilon$  solver method as iteration proceeds.

SIMPLE. First Order Upwind was chosen for discretization. The solution has been initialized from all zones. Iterations were carried out for the optimal time step size of 0.03 second. Fig. 4 shows the residual plot for the  $k-\epsilon$  solver method as the iteration proceeds.

## RESULTS AND DISCUSSION

### Analytical model testing

This model was tested with pressure measurements from a well drilled with aerated fluids. A vertical well was drilled in Northern Africa. The borehole profile is described by a 9-5/8 in. intermediate casing run from the surface to 7632 ft. Below the intermediate casing is a 7 in. production liner tied back to the intermediate casing at 7304 ft. The liner was run from 7304 ft to 8859 ft. An open hole was drilled out of the bottom of the liner to a depth of 9571 ft. Then, aerated fluid was used to reduce the bottom hole pressure and allow underbalanced drilling. The open hole interval (from 8859 ft to 9571 ft) was drilled with a 6 in. Tricone roller cutter drill bit. The drill string, while drilling at a depth of approximately 9381 ft, was made up of 5 in. drill pipe from the surface to 7361 ft; 3-1/2 in. drill pipe from 7361 to 8361 ft; 3-1/2 in. heavyweight drill pipe from 8361 to 8841 ft; and 4-3/4 in. collars from 8841 to 9381 ft. The incompressible fluid was 8.60 ppg treated-water, which was injected at a rate of 45 gpm. The gas was inert atmospheric air with an injection volumetric flow rate of approximately 1500 acfm (cubic feet per minute of actual air, at surface elevation location of approximately 3700 ft). The back pressure at the choke manifold was kept at about approximately 600 psig.

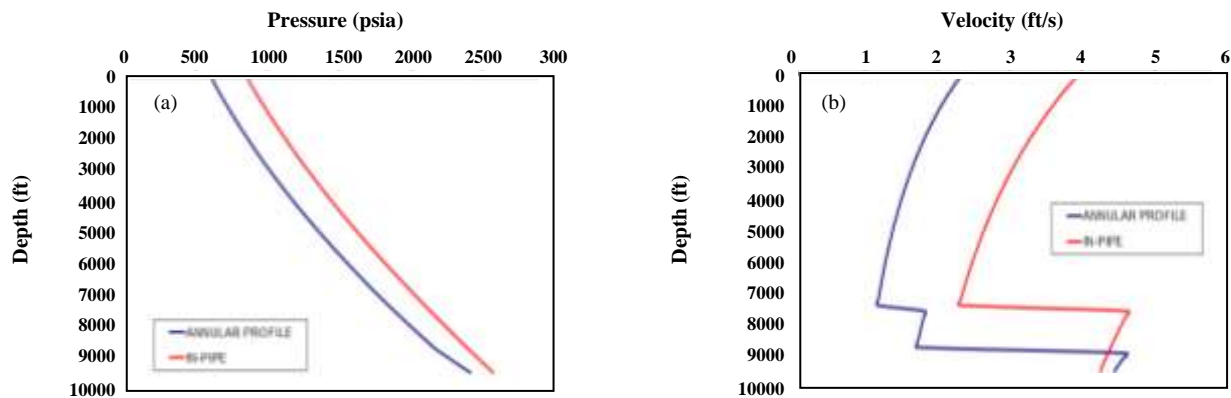


Fig. 5: a) Pressure and b) velocity profiles inside the drill string, annulus and through the bit in the tested well.

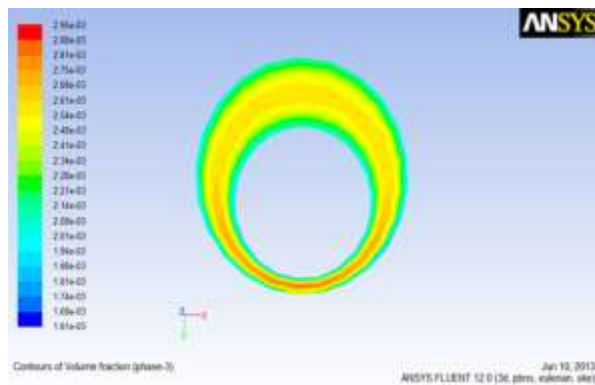


Fig. 6: Contours of the volume fraction of solid in the outlet of the annulus at an inlet water velocity of 1.5338 m/s and inlet air velocity of 0.6767 m/s for ROP of 80 ft/h.

Accurate prediction of a shut-in and flowing bottom hole pressures in inclined holes present a challenge in UBD. It is highly desirable to develop a simple and accurate hydraulics equation for this purpose. The analytical Equation (7) was used in this work on the basis of Guo *et al.*'s (2003) work [33]. By applying Eq. (7) to borehole segments, the bottom hole pressure was found to be 2189 psig. The actual bottom hole pressure was approximately 2000 psig. The obtained error through this equation was 8.66% in this case.

$$b(P - P_s) + \frac{1 - 2bM}{2} \ln \left| \frac{(P + M)^2 + N}{(P_s + M)^2 + N} \right| - \quad (7)$$

$$\frac{M + \frac{b}{c}N - bM^2}{\sqrt{N}} \left[ \tan^{-1} \left( \frac{P + M}{\sqrt{N}} \right) - \tan^{-1} \left( \frac{P_s + M}{\sqrt{N}} \right) \right] =$$

$$a(\cos\theta + d^2e)L$$

The trends for the test model, as shown in Fig. 5, were used to obtain the pressure and velocity profile in the well.

#### Steady state three phase flow simulation with CFD

Fig. 6 shows the contours of volume fraction of solid in the outlet of the annulus at an inlet water velocity of 1.5338 m/s and inlet air velocity of 0.6767 m/s for ROP of 80 ft/hr after the steady state is achieved. The colour scale given to the left of each contour indicates the value of volume fraction corresponding to the colour. In general, increasing the pipe rotation in the low angle wells increases the concentration of cutting in the wells and it is not the right way for cutting removal in this type of wells. On the other hand, by increasing the inclination, pipe rotation is becoming more effective for cutting transport in wells. So, the cutting concentration decreases with increasing the pipe rotation. Eventually, the pipe rotation can be considered as an effective way for hole cleaning in the highly inclined wells. In the high angle wells, the pipe rotation moves the cutting from the cutting bed to the high side of the annulus and put the cutting along with the mixture flow. This phenomenon improves the cutting transport efficiency in the high angle wells. On the other hand, in low inclinations, increasing the pipe rotational speed as well as increasing the turbulence causes the particles to be trapped in the annulus and decreasing the cutting transport efficiency.

Counters of velocity magnitude of water and air in the outlet obtained at an inlet water velocity of 1.5338 m/s and inlet air velocity of 0.6767 m/s for ROP of 80 ft/h are shown in Fig. 7.

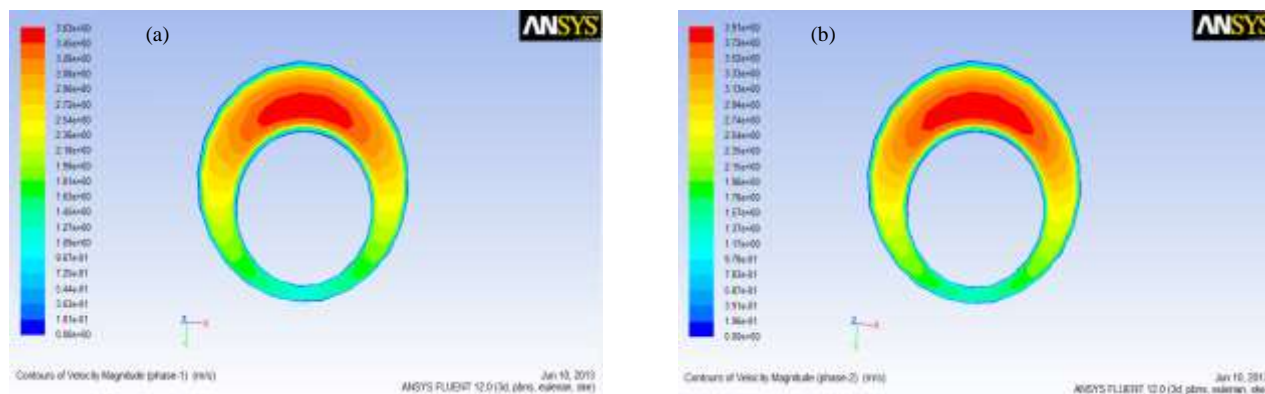


Fig. 7: Counters of a) water and b) air velocities magnitude in the outlet.

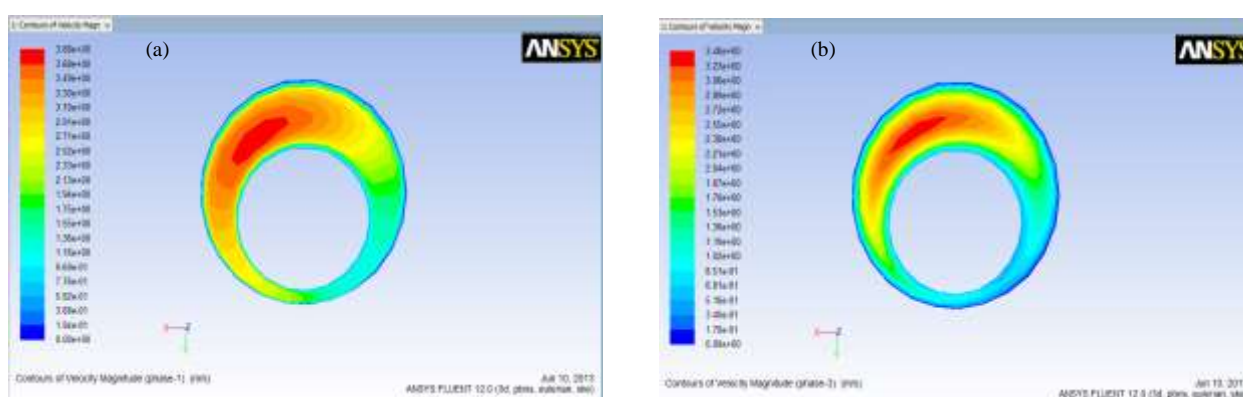


Fig. 8: Contour of a) water and b) solid particle axial velocities in an eccentric annulus (0.65 eccentricities, 11 rad/s rotation).

It can be seen from Fig. 8 that the volume fraction of solid in the narrow side of the annulus is more than the wider side due to the gravity effect. The velocity of water and solid show difference in the shape of their velocity curves (the velocity profile across any given section of pipe). In turbulent flow, the fairly flat velocity distribution of water exists across the annulus. However, the velocity distribution of solid is not flat.

Fig. 9 shows the comparison of pressure between the predicted data and that measured by *Osgouei* in reference [30]. As this figure shows, the estimated values are very close to the experimental value of pressure, representing the accuracy of the CFD model.

The particle size of the solid phase was taken in the range of 0.001 m to 0.004 m to investigate the effect of particle size on pressure drop. The simulation results obtained are shown in Fig. 10. This figure illustrates that outlet pressure shows an increasing trend as the particle size is increased for a particular air and water velocity.

The inside pipe rotation was taken in the range of 2 rad/s to 11 rad/s to investigate the effect of pipe rotation on pressure drop. The obtained simulation results are shown in Fig. 11. The figure illustrates that by increasing pipe rotation rate, the pressure drop was not considerably changed in this simulation, as the cuttings injection, liquid, and gas flow rates are kept constant. *Amanna* and *Movaghar* (2016) [34] investigated the effects drill pipe rotation on cutting transport in which increasing in values of flow rate and drill pipe rotation was effectively improved the drag effects leading to superior cutting removal. In the current investigation, the liquid and gas flow rates were kept constant so that pressure drop did not change sensibly.

#### Transient three-phase flow simulation with CFD

The inlet air velocity was changed from 0.6767 m/s to 1.5338 m/s to investigate its effect on pressure drop. The obtained simulation results are shown in Fig. 12. A change in outlet pressure is seen in the annulus during

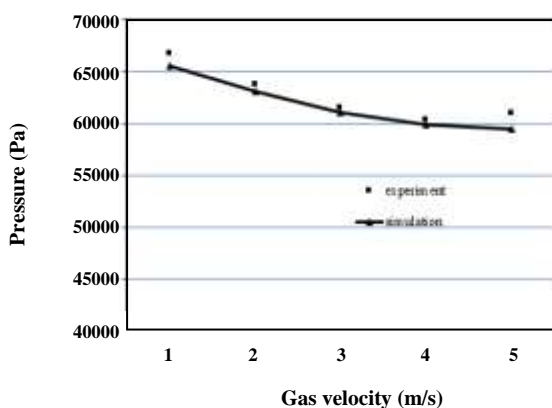


Fig. 9: Comparison of the predicted pressure of eccentric annulus data and data measured by Osgouei in Ref. [30].

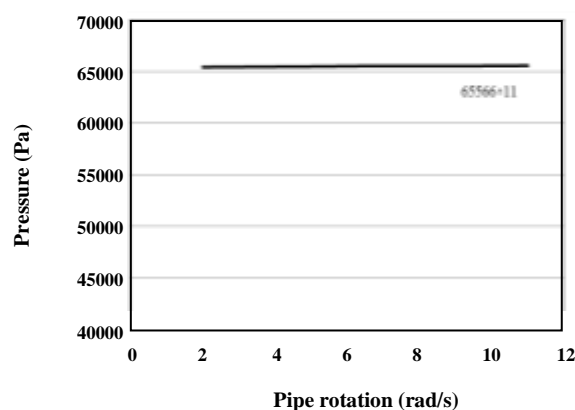


Fig. 11: Effect of pipe rotation on pressure drop.

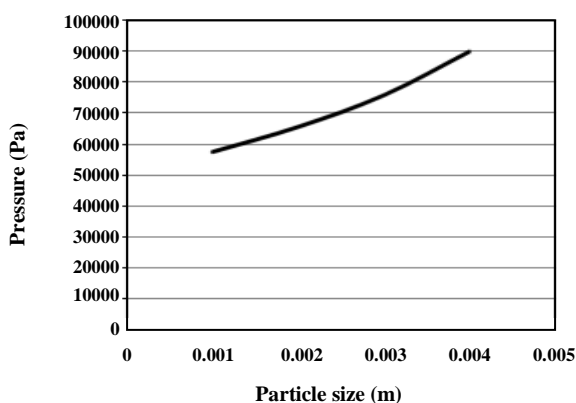


Fig. 10: Effect of particle size on pressure drop.

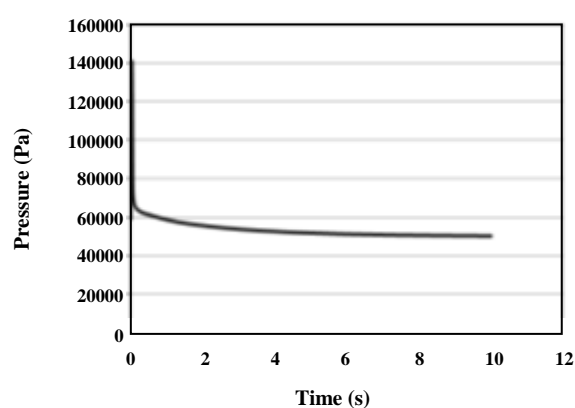


Fig. 12: Pressure variations versus time through increasing air velocity.

the simulation, but after some time no significant change was observed indicating that the quasi steady state has been reached. Simulations were carried out until there was no change in the pressure drop. From the figure, it is very clear that there were pressure changes for the first 10 sec after which, there was no subsequent change in the pressure even though the simulation continued.

Fig. 12 also illustrates that by increasing air velocity, pressure increases suddenly because of a change in movement inertia. The pressure, then, decreased suddenly, but then reduction was slowly during the next 10 seconds. After which, there was no subsequent change in the pressure even though the simulation went on. In this regards, the effects of the solid fraction with time was investigated in which firstly increased then, when time goes on the solid fraction was decreased. On the other hand, in high flow rates of air, escalating the drill pipe rotation caused the enhancing of solid fraction.

## CONCLUSIONS

The success of a UBD operation relies on maintaining the wellbore pressure within an optimized window that typically depends on a UBD pressure system designed by a computer program. Analytical models are used for the simple geometry, and some assumptions are considered and developed to obtain the solution. Numerical simulations for three-phase flow in annulus were performed using the transient Eulerian model with the CFD packages, ANSYS Fluent 12. The turbulence was described using the k- $\epsilon$  model.

It was observed that pressure drop is significantly increased with increasing solid particle size. Simulations showed that the pressure drop remains almost constant with the rotation of the inner pipe. The results revealed that CFD has excellent potential to simulate three-phase flow systems. CFD simulations showed that the velocity sharply decreased with radius in a region close

to the inner pipe, and then gradually dropped to zero at the outer casing wall. The axial velocity profile for the 0.65 eccentricity annulus showed that most fluid flows through the wider gap side. The axial velocity of water and solids at the narrow gap side was close to zero, even with a high pipe rotary speed. However, in a low eccentricity annulus where the narrower side becomes wider, pipe rotation can bring more fluid particles through the narrow gap during a certain period of time.

### Nomenclatures

#### Abbreviations

UBD	Underbalanced Drilling
OBD	Overbalanced Drilling
CFD	Computational Fluid Dynamics
FDM	Finite Difference Method
FEM	Finite Element Method
FVM	Finite Volume Method
E-L	Eulerian-Lagrangian
k- $\epsilon$	Reynolds Stress Model
VOF	Volume of Fluid Method
bbl	Barrel

#### English Symbols

$D_p$	Outer pipe diameter
$D_w$	Well diameter
$v_L$	Liquid velocity
$v_G$	Gas velocity
$v_{SL}$	Superficial liquid velocity
$v_{SG}$	Superficial gas velocity
$v_m$	Mixture velocity
$T$	Temperature
$P_2$	Bottom hole pressure
$Q_l$	Liquid flow rate
$Q_g$	Gas flow rate
$Re$	Reynolds number
$R$	Gas constant
$d_b$	Bit diameter
$S_s$	Solid specific gravity, water = 1
ROP	Rate of penetration, ft/hour
$S_g$	Specific gravity of gas, air = 1
$S_{gf}$	Specific gravity of gas influx, air = 1
$\theta$	Inclination angle, degree

#### Greek letters

$\alpha$	Gas fraction
----------	--------------

$\rho_l$	Liquid density
$\rho_g$	Gas density
$\rho_m$	Mixture density
$\mu_m$	Mixture viscosity

Received: Jun. 6, 2017 ; Accepted : Dec. 12, 2017

### REFERENCES

- [1] Guo B., Use of Spreadsheet and Analytical Models to Simulate Solid, Water, "Oil and Gas Flow in Underbalanced Drilling", *Middle East Drilling Technology Conference*, 22-24 October (2001), Bahrain, SPE-72328-MS
- [2] Perez-Tellez C., Smith J.R., Edwards J.K., "A New Comprehensive Mechanistic Model for Underbalanced Drilling Improves Wellbore Pressure Predictions", *SPE International Petroleum Conference and Exhibition*, 10-12 February (2003), Mexico, SPE-74426-MS
- [3] Bennion D.B., Thomas F.B., Bietz R.F., Bennion D.W., *Underbalanced Drilling: Praises and Perils*, *SPE Drilling and Completion*, **13**(4): SPE-52889-PA (1998).
- [4] Soleymani M., Kamali M.R., Saeedabadian Y., *Experimental Investigation of Physical and Chemical Properties of Drilling Foam and Increasing its Stability*, *Iran J. Chem. Chem. Eng.(IJCCE)*, **32**(3): 127-132 (2013).
- [5] Ekambara K., Sanders R.S., Nandakumar K., Masliyah J.H., *CFD Simulation of Bubbly Two-Phase Flow in Horizontal Pipes*, *Chem. Eng. J.*, **144**(2): 277-288 (2008).
- [6] Vieira P., "Determination of Minimum Water-Air Rates Required for Effective Cuttings Transport in High Angle and Horizontal Wells", M.Sc. Thesis, University of Tulsa, (2000).
- [7] Rodriguez P.V., "Experimental Determination of Minimum Air and Water Flow Rates for Effective Cutting Transport in High Angle and Horizontal Wells", M.Sc. Thesis, University of Tulsa (2001).
- [8] Vieira P., Miska S., Reed T., Kuru E., "Minimum Air and Water Flow Rates Required for Effective Cuttings Transport in High Angle and Horizontal Wells", *IADC/SPE Drilling Conference*, 26-28 February (2002), Dallas, Texas, SPE-74463-MS

- [9] Doan Q.T., Oguztoreli M., Masuda Y., Yonezawa T., Kobayashi A., Naganawa S., Kamp A., **Modeling of Transient Cuttings Transport in Underbalanced Drilling (UBD)**, *SPE J.*, **8**(2): 160-170 (2003).
- [10] Zhou L., Ahmed R.M., Miska S.Z., Takach N.E., Yu M., Saasen A., “**Hydraulics of Drilling with Aerated Muds under Simulated Borehole Conditions**”, *SPE/IADC Drilling Conference*, 23-25 February (2005), Amsterdam, Netherlands, SPE-92484-MS
- [11] Lourenco A.M.F., Nakagawa E.Y., Martins A.L., Andrade P.H., “**Investigating Solids-Carrying Capacity for an Optimized Hydraulics Program in Aerated Polymer-Based- Fluid Drilling**”, *SPE Drilling Conference*, 21-23 February (2006), Miami, Florida, USA, SPE-99113-MS
- [12] Zhange J., Zhang Y., Hu L., Zhang J., Chen G., **Modification and Application of a Plant Gum as Eco-Friendly Drilling Fluid Additive**, *Iran J. Chem. Chem. Eng.(IJCCE)*, **34**(2): 103-108 (2015).
- [13] Zhou L., **Hole Cleaning During Underbalanced Drilling in Horizontal and Inclined Wellbore**, *SPE Drilling & Completion*, **23**(3): 267-273 (2008), SPE-98926-PA
- [14] Bourgoynne Jr. A.T., “**Well Control Considerations for Underbalanced Drilling**”, *SPE Annual Technical Conference and Exhibition*, 5-8 October (1997), San Antonio, Texas, SPE-38584-MS
- [15] Saponja J., **Challenges with Jointed Pipe Underbalanced Operations**, *SPE Drilling & Completion*, **13**(2): (1998), SPE-37066-PA
- [16] Brennen C.E., “**Fundamentals of Multiphase Flows**”, Cambridge University Press, 1st ed., (2009).
- [17] Wallis G.B., “**One-Dimensional Two-Phase Flow**”, McGraw-Hill, 1st ed, (1969).
- [18] ANSYS Fluent 12.1 Theory Guide, (2010).
- [19] Khezrian M., Hajidavalloo E., Shekari Y., **Modeling and Simulation of Under-Balanced Drilling Operation Using Two-Fluid Model of Two-Phase Flow**, *Chem. Eng. Res. Des.*, **93**: 30-37 (2015).
- [20] Shekari Y., Hajidavalloo E., Behbahani-Nejad M., **Reduced Order Modeling of Transient Two-Phase Flows and Its Application to Upward Two-Phase Flows in the Under-Balanced Drilling**, *Appl. Math. Comput.*, **224**: 775-790 (2013).
- [21] Ghobadpouri S., Hajidavalloo E., Noghrehabadi A.M., **Modeling and Simulation of Gas-Liquid-Solid Three-Phase Flow in Under-Balanced Drilling Operation**, *J. Pet. Sci. Eng.*, **156**: 348-355 (2017).
- [22] Moradi F., Kazemeini M., Fattahi M., **A Three Dimensional CFD Simulation and Optimization of Direct DME Synthesis in a Fixed Bed Reactor**, *Pet. Sci.*, **11**(2): 323-330 (2014).
- [23] Versteeg H.K., Malalasekera W., “**An Introduction to Computational Fluid Dynamics: The Finite Volume Method**”, 2nd ed., Pearson, (2007).
- [24] Hirt C.W., Nichols B.D., **Volume of Fluid (VOF) Method for the Dynamics of Free Boundaries**, *J. Comput. Phys.*, **39**: 201-225 (1981).
- [25] Keshavarz Moraveji M., Sabah M., Shahryari A., Ghaffarkhah A., **Investigation of Drill Pipe Rotation Effect on Cutting Transport with Aerated Mud Using CFD Approach**, *Adv. Powder Technol.*, **28**(4): 1141-1153 (2017).
- [26] Azizi S., Hosseini S.H., Ahmadi G., Moravej M., **Numerical Simulation of Particle Segregation in Bubbling Gas-fluidized Beds**, *Chem. Eng. Technol.*, **33**: 421-432 (2010).
- [27] Moraveji M.K., Sokout F.S., Rashidi A., **CFD Modeling and Experimental Study of Multi-walled Carbon Nanotubes Production by Fluidized Bed Catalytic Chemical Vapor Deposition**, *Int. Commun. Heat Mass Transfer*, **38**: 984-989 (2011).
- [28] Lun C.K.K., Savage S.B., Jeffrey D., Chepurniy N., **Kinetic Theories for Granular Flow: Inelastic Particles in Couette Flow and Slightly Inelastic Particles in a General Flowfield**, *J. Fluid Mech.*, **140**: 223–256 (1984).
- [29] Gidaspow D., Bezburuah R., Ding J., **Hydrodynamics of Circulating Fluidized Beds: Kinetic Theory Approach**, Illinois Institute of Technology, Chicago IL (United States), Department of Chemical Engineering (1991).
- [30] Ettehadi Osgouei R., “**Determination of Cuttings Transport Properties of Gasified Drilling Fluids**”, The Graduate School of Natural and Applied Sciences of Middle East Technical University, Ph.D. Thesis (2010).
- [31] Epelle E.I., Gerogiorgis D.I., **A Multiparametric CFD Analysis of Multiphase Annular Flows for Oil and Gas Drilling Applications**, *Comput. Chem. Eng.*, **106**: 645-661 (2017).

- [32] “ANSYS Fluent 12.0 User’s Guide”, Interphase Exchange Coefficients (2016).
- [33] Guo B., Sun K., Ghalambor A., Xu C., [A Closed Form Hydraulics Equation for Aerated Mud Drilling in Inclined Wells](#), *SPE Drilling & Completion*, **19**(2): (2004), SPE-88840-PA
- [34] Amanna B., Khorsand Movaghar M.R., [Cuttings Transport Behavior in Directional Drilling Using Computational Fluid Dynamics \(CFD\)](#), *J. Nat. Gas Sci. Eng.*, **34**: 670-679 (2016).